Ultrasonics Sonochemistry 36 (2017) 301–308

Contents lists available at ScienceDirect

Ultrasonics Sonochemistry

journal homepage: www.elsevier.com/locate/ultson

Wastewater treatment by sonophotocatalysis using PEG modified TiO_2 film in a circular Photocatalytic-Ultrasonic system

Xiaohong Hu [a], Qi Zhu [a], Zhibin Gu [a], Nan Zhang [a], Na Liu [a], Mishma S. Stanislaus [a], Dawei Li [a], Yingnan Yang [b,*]

[a] Graduate School of Life and Environmental Sciences, University of Tsukuba, 1-1-1 Tennoudai, Tsukuba, Ibaraki 305-8577, Japan
[b] Faculty of Life and Environmental Sciences, University of Tsukuba, 1-1-1 Tennoudai, Tsukuba, Ibaraki 305-8577, Japan

ARTICLE INFO

Article history:
Received 2 September 2016
Received in revised form 5 December 2016
Accepted 5 December 2016
Available online 8 December 2016

Keywords:
Wastewater treatment
PEG modified TiO_2 film
Sol-gel method
Photocatalytic-Ultrasonic system

ABSTRACT

TiO_2 photocatalyst film recently has been utilized as the potential candidate for the wastewater treatment, due to its high stability and low toxicity. In order to further increase the photocatalytic ability and stability, different molecular weight of polyethylene glycol (PEG) were used to modify TiO_2 structure to synthesize porous thin film used in the developed Photocatalytic-Ultrasonic system in this work. The results showed that PEG2000 modified TiO_2 calcinated under 450 °C for 2 h exhibited the highest photocatalytic activity, attributed to the smallest crystallite size and optimal particle size. Over 95.0% of rhodamine B (Rh B) was photocatalytically degraded by optimized PEG_{2000}-TiO_2 film after 60 min of UV irradiation, while only about 50.8% of Rh B was decolored over pure TiO_2 film. Furthermore, optimized PEG_{2000}-TiO_2 film was used in a circular Photocatalytic-Ultrasonic system, and the obtained synergy (0.6519) of sonophotocatalysis indicated its extremely high efficiency for Rh B degradation. In this Photocatalytic-Ultrasonic system, larger amount of PEG_{2000}-TiO_2 coated glass beads, stronger ultrasonic power and longer experimental time could result to higher degradation efficiency of Rh B. In addition, repetitive experiments showed that about 97.2% of Rh B were still degraded in the fifth experiment by sonophotocatalysis using PEG_{2000}-TiO_2 film. Therefore, PEG_{2000}-TiO_2 film used in Photocatalytic-Ultrasonic system has promising potential for wastewater treatment, due to its excellent photocatalytic activity and high stability.

1. Introduction

In order to develop efficient methods for wastewater treatment, advanced oxidation processes (AOPs) have attracted much attention over the past decades, involving various combinations of ozone, hydrogen peroxide, sonolysis, ultraviolet (UV) radiation, and photocatalysis [1–6]. Of various AOPs, photocatalysis is the most promising technology, because large number of free radicals could be generated during photocatalytic process, and those reactive radicals almost have no selectivity to completely degrade refractory organic matters in wastewater. Recently, sonolysis, another AOP, has been considerably studied to degrade organics, and it's reported that ultrasound irradiation could also lead to the formation of reactive species, such as ·OH radicals [7–9]. This formation takes place in the cavity in the present of ultrasound due to the localized temperatures (5000 K) and pressures (1000 atm) [10]. More importantly, the combination of sonolysis and photocatalysis, namely sonophotocatalysis has showed enhanced efficiency to deeply degrade various organics, as their synergistic effect could largely enhance the degradation efficiency of refractory organics [11–14]. However, there were limited reports about development of sonophotocatalysis system for wastewater treatment.

As we all known, TiO_2 photocatalyst film has been found application in wastewater treatment due to its low toxicity [15–17], and it can be prepared by many techniques including sputtering, chemical vapor deposition, sol–gel deposition and spray pyrolysis [18–23]. However, the photocatalytic ability of photocatalyst film largely depends on its crystal structure, crystallite size, surface area, thickness and porosity [24–28]. And the photocatalytic activity of TiO_2 still need to be improved, mainly because of its large band gap and large crystallite size [29,30]. As we all know, PEG is a traditional pore-forming agent, and commonly used for the synthesis of porous thin film [31–33]. Besides, PEG modification could affect the crystal structure and particle size of TiO_2, which further has effluence on its photocatalytic ability [34,35]. Utile now, there

* Corresponding author.
E-mail address: yo.innan.fu@u.tsukuba.ac.jp (Y. Yang).

http://dx.doi.org/10.1016/j.ultsonch.2016.12.008
1350-4177/

is few research focusing on optimization and application of different PEG molecule weight modified TiO_2 film, especially for developing a sonophotocatalytic water-treatment system. Therefore, different PEG molecule weight (300, 2000, 6000 and 20,000) modified TiO_2 (PEG-TiO_2) film coated on glass beads could be utilized for developing a novel system, in which sonophotocatalysis can be conducted for wastewater treatment.

In this study, PEG-TiO_2 powders were firstly synthesized using different PEG molecular weights by sol-gel method. Rh B degradation, crystal structures, optical properties and morphologies were evaluated to compare different molecular weights of PEG modified TiO_2. Then PEG-TiO_2 (using optimal PEG molecular weight and addition level) films on glass beads were synthesized by varying calcination temperature, calcination time and coating layers. Next, sonocatalysis, photocatalysis and sonophotocatalysis were carried out through Rh B degradation using optimized PEG-TiO_2 film in a circular Photocatalytic-Ultrasonic system developed in this work. Besides, different ultrasonic power and time were investigated on Rh B degradation efficiency. Finally, the sonophotocatalytic mechanism of PEG-TiO_2 was finally proposed to deeply understand Rh B degradation processes.

2. Experimental

2.1. Materials

All reagents were of analytical purity and were used without further purification. Tetrabutyl titanate [$Ti(OC_4H_9)_4$] (99.5%) and ethanol were used as TiO_2 source and solvent, respectively. PEG with different average molecular weight of 300, 2000, 6000 and 20,000 was used, respectively, to synthesize PEG_{300}-TiO_2, PEG_{2000}-TiO_2, PEG_{6000}-TiO_2 and PEG_{2000}-TiO_2 samples. Rhodamine B (Rh B) was used as a model of organic to evaluate the photocatalytic efficiency for wastewater treatment. All of the agents were obtained from Wako Pure Chemical Industries, Ltd, Japan.

2.2. Preparation of different PEG-TiO_2 powders and films

2.2.1. Tetrabutyl titanate solution

At first, 20 ml tetrabutyl titanate was dissolved in 90 ml ethanol under vigorous stirring for 20 min at ambient temperature to obtain a transparent solution. A certain amount of different PEG (300, 2000, 6000 and 20,000) were dissolved in 6 ml of 1 m/L HNO_3 solution, and was added drop-wise into the transparent tetrabutyl titanate solution. Amount of PEG was 0, 1, 2, 3 and 4 g/L, respectively. After stirring for 12 h at room temperature, the final transparent, homogeneous and stable sol was obtained.

2.2.2. PEG-TiO_2 powder

The above prepared sol was dried under 105 °C for 24 h, and calcined at 450 °C for 2 h in a muffle furnace to obtain photocatalyst powders, which were labeled as PEG_{MW}-TiO_2 (MW = 300, 2000, 6000 20,000), where MW represents different PEG molecular weights. Pure TiO_2 without PEG was synthesized at the same conditions as the control.

2.2.3. PEG_{2000}-TiO_2 film on glass beads

As above mentioned, transparent tetrabutyl titanate sol was prepared by using 3 g/L of PEG2000. For the synthesis of PEG_{2000}-TiO_2 films, glass beads (φ: 3 mm) were employed as substrate for the coating. Prior to coating, glass beads were thorough cleaned with deionized water and ethanol by using ultrasonic treatment, and was dried in the air. Then, the glass beads were coated by the prepared sol and dried under 105 °C for 24 h, and calcined in a muffle furnace at 300, 350, 400, 450 and 500 °C at time of 0.5, 1.0, 1.5, 2.0, 2.5 and 3.0 h, respectively. The coating and calcination processes were repeated to obtain 1, 2, 3 and 4-layer films.

2.3. Characterization

X-ray diffraction (XRD) patterns of photocatalyst was characterized by using a Rigaku Altima III Rint-2000 X-ray Diffractrometer equipped with Cu Kα radiation (λ = 1.54178 Å). The morphologies of photocatalysts were observed by scanning electron microscopy (SEM, Hitachi FE-SEM S-4800 EDX). UV–vis diffusion reflectance spectra were recorded on a JASCO V-570 spectrophotometer with a wavelength range of 220–800 nm and converted to absorption spectra by the standard Kubelka-Munk method. The photoluminescence (PL) spectra with an excitation wavelength of 325 nm were recorded with a JASCO FP8500 fluorescence spectrophotometer. Rh B degradation was conducted by using UV light (irradiation intensity: 12.8 W/m^2).

2.4. Novel Photocatalytic-Ultrasonic system for Rh B degradation

2.4.1. Photocatalytic reactor

Photocatalytic reactor was developed by a long glass tube (outside diameter: 10 mm, inside diameter: 6 mm, thickness: 2 mm, length: 335 mm) filled up with PEG_{2000}-TiO_2 film coated glass beads (or uncoated glass beads) and 2 mg/L of Rh B solution. An UV black light lamp (Tokyo Metal BM-10BLB, length: 300 mm, diameter: 28 mm, power: 10 W, λ max: 365 nm) was fixed above the glass tube at a distance of 150 mm. The average light intensity in the photocatalytic reactor (12.8 W/m^2) was measured by an UV light meter (UV340, CUSTOM, Japan).

2.4.2. Ultrasonic reactor

Ultrasonic reactor was constructed by an ultrasonic bath and a glass tube filled up with PEG_{2000}-TiO_2 film coated glass beads (or uncoated glass beads) (φ: 3 mm). An ultrasonic bath (AU-50C) has the power of 120 W and frequency of 28 kHz. Another ultrasonic bath (B200) shows the power of 30 W and frequency of 30 Hz.

2.4.3. Photocatalytic-Ultrasonic system

Photocatalytic-Ultrasonic system combined of photocatalytic reactor and sonocatalytic reactor as shown in Fig. 1. All of sonocatalytic, photocatalytic and sonophotocatalytic processes can be carried out in this novel Photocatalytic-Ultrasonic system under different conditions. 100 mL of Rh B solution cyclically flowed in this system through pump and 5 ml of suspension was collected every 30 min, and then centrifuged (10,000 rpm) to remove photocatalysts. Then the upper clear liquid was analyzed to evaluate the concentration of Rh B by a spectrophotometer (UV-1600,

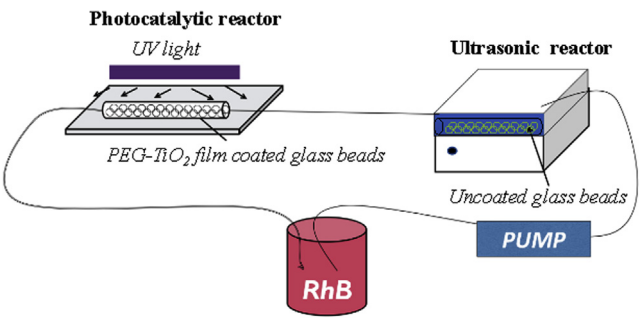

Fig. 1. Schematic of the circular Photocatalyst-Ultrasonic system.

Shimadzu) at a wavelength of 554 nm which corresponds to the maximum absorption wavelength of Rh B.

3. Results and discussion

3.1. Crystal structural and morphological properties of PEG_{MW}-TiO_2 photocatalysts

XRD patterns of different PEG_{MW}-TiO_2 photocatalysts were shown in Fig. 2. It can be found that the pure TiO_2 exhibited the mixture of anatase phase (JCPDS file No.00-021-1272) and rutile phase (JCPDS file No.00-021-1276) [36]. The peaks located at 25.28°, 37.80° and 48.05° were ascribed to anatase phase, while those peaks at 27.45°, 36.09° and 44.05° were attributed to rutile phase. Obviously, PEG (300, 2000, 6000 and 20,000) modified TiO_2 showed weaker intensity of rutile phase [37], compared with pure TiO_2. There was no rutile phase found in PEG_{2000}-TiO_2 and PEG_{300}-TiO_2. As we all know, rutile phase has lower photocatalytic ability than anatase phase [36]. The average crystallite size was calculated by Halder-Wagner method and summarized in Table 1. Pure TiO_2 possessed the largest crystallite size (18.4 nm), while after PEG modified, their crystallite sizes were decreased [38,39]. PEG_{2000}-TiO_2 had the smallest crystallite size of 8.5 nm. Usually, the decreased content of rutile phase contributes to the decrease of crystallite size, finally leading to the higher photocatalytic ability [36]. Fig. 3 showed UV–vis spectra of different photocatalysts, and it can be found that PEG modified TiO_2 had a blue shift compare to pure TiO_2. According to XRD results (Fig. 2), PEG (300, 2000, 6000 and 20,000) modified TiO_2 showed much weaker intensity of rutile phase, compared with pure TiO_2. Therefore, the majority of components in PEG modified TiO_2 was anatase phase. As we all know, anatase phase has a little higher band gap (3.20 eV) than that of rutile phase (3.13 eV), which leads to a little blue shift of anatase phase in UV–vis spectra compared to rutile phase. Therefore, PEG modified TiO_2 had a blue shift compare to pure TiO_2.

Then morphologies of different PEG_{MW}-TiO_2 photocatalyst powders were observed using SEM (Fig. 4a–e). It could be found that as-prepared photocatalysts were homogeneous nanoparticles. Pure TiO_2 showed the smallest particle size of 18 nm, while after modification with different PEG molecules, particle size increased with the increase of PEG molecular weight [37]. PEG_{300}-TiO_2, PEG_{2000}-TiO_2, PEG_{6000}-TiO_2 and PEG_{20000}-TiO_2 had average particle size of 54, 98,162 and 230 nm respectively. It's reported that photocatalytic ability of TiO_2 increases with the increase of particle size to the optimal value, but it decreases when particle size further increases [28].Generally, the density of recombination center decreases when the particle size increases, which hinders the recombination of electrons and holes. In addition, when the particle size decreases under a certain value, the quantization effect would result in the increase of band gap, finally leading to reduce of photocatalytic activity [28]. Besides, the specific surface areas of different materials were measured and summarized in Table 1. It could be found that specific surface areas of TiO_2, PEG_{300}-TiO_2, PEG_{2000}-TiO_2, PEG_{6000}-TiO_2 and PEG_{20000}-TiO_2 were 19.42, 35.32, 38.85, 30.75 and 52.10 m^2/g, respectively. Therefore, PEG-TiO_2 showed higher specific surface area than pure TiO_2. As we all know, photocatalysts with higher specific surface area usually have higher photocatalytic activity. Therefore, PEG modified TiO_2 should show higher photocatalytic activity, due to more anatase content, larger particle size and higher specific surface area.

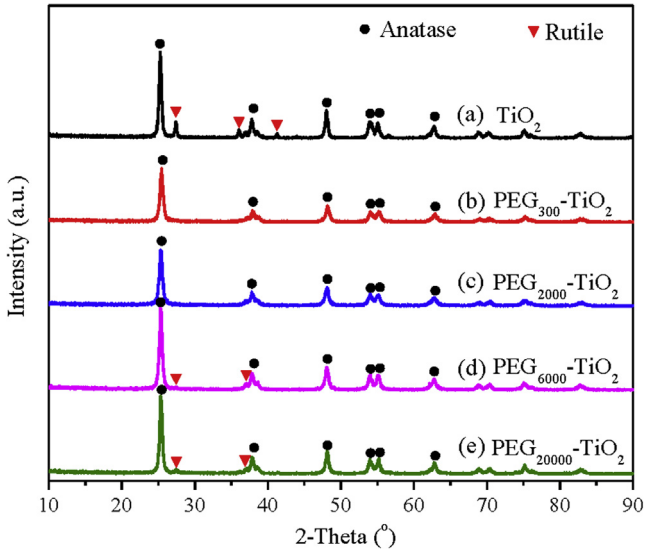

Fig. 2. XRD patterns of (a) Pure TiO_2, (b) PEG_{300}-TiO_2, (c) PEG_{2000}-TiO_2, (d) PEG_{6000}-TiO_2 and (e) PEG_{20000}-TiO_2.

3.2. Photocatalytic degradation of Rh B by PEG_{MW}-TiO_2 photocatalysts

In order to investigate photocatalytic activities of as prepared PEG_{MW}-TiO_2 photocatalysts, 2 mg/L of Rh B solution (100 ml) was degraded by 0.10 g of different PEG_{MW}-TiO_2 powders under irradiation of simulated UV light (Irradiation intensity: 12.8 W/m^2). Results indicated that in comparison with pure TiO_2, PEG_{MW}-TiO_2 showed better photocatalytic degradation performance (Fig. 5a). And PEG_{2000}-TiO_2 exhibited the highest efficiency than PEG_{300}-TiO_2, PEG_{6000}-TiO_2 and PEG_{20000}-TiO_2. About 92.2% of Rh B was decolored by PEG_{2000}-TiO_2 after 120 min of irradiation, while only 33.4% of Rh B was degraded by pure TiO_2. The first-order kinetic model was used to describe the kinetics of Rh B degradation, and the results were shown in Fig. 5b and Table 2. According to the first-order reaction model, the apparent rate constant, k_{app} (min^{-1}) is determined from regression curves of $-\ln(C/C_0)$ versus irradiation time (min). The apparent rate constants of PEG_{MW}-TiO_2 were also much higher than pure TiO_2. k_{app} was 0.00046 min^{-1} for Rh B degradation over pure TiO_2, while in case of PEG_{2000}-TiO_2 it showed the highest value of 0.00093. Therefore, PEG_{2000}-TiO_2 photocatalyst exhibited enhanced photocatalytic ability under simulated UV light irradiation, due to its smallest crystallite size and optimal particle size. In addition, influence of different amount of PEG2000 on photocatalytic activity was demonstrated (Fig. 6). It indicated that photocatalytic ability first increased and then decreased with the increase of PEG amount, and TiO_2 modified with 3 g/L of PEG2000 showed the highest photocatalytic activity.

3.3. Optimization of PEG_{2000}-TiO_2 photocatalyst film

According to the previous results that TiO_2 powder modified with PEG2000 showed the highest photocatalytic ability than others, therefore PEG_{2000}-TiO_2 film should be optimized to develop highly efficient photocatalytic film. Then the influences of calcination temperature, calcination time and coating layers on PEG_{2000}-TiO_2 film were systematically investigated through Rh B degradation. It was found that calcination temperature had significant influence on photocatalytic activity. The degradation efficiency of Rh B firstly increased with the increase of calcination temperature from 300 to 450 °C, while it decreased when temperature over 450 °C (Fig. 7a). It was due to the change of crystal phase between rutile and anatase. Usually, anatase phase would be formed around 400 °C, which exhibited higher photocatalytic activity than rutile phase, while rutile phase is transferred from anatase phase when temperature over 450 °C [36], leading to the decrease of photocatalytic ability.

Table 1
Properties of different photocatalysts.

	Pure TiO_2	PEG_{300}-TiO_2	PEG_{2000}-TiO_2	PEG_{6000}-TiO_2	PEG_{20000}-TiO_2
Crystallite size (nm)	18.4	14.5	8.5	10.4	14.7
Specific surface area (m^2/g)	19.42	35.32	38.85	30.75	52.10

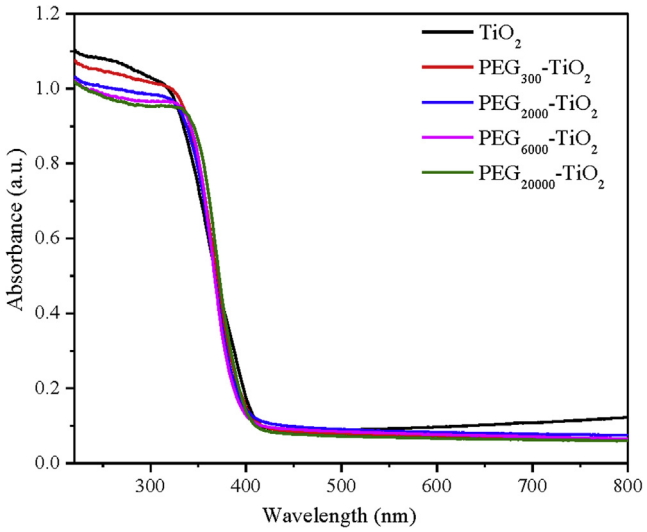

Fig. 3. UV–vis diffusive reflectance spectra of pure-TiO_2, PEG_{300}-TiO_2, PEG_{2000}-TiO_2, PEG_{6000}-TiO_2 and PEG_{20000}-TiO_2.

Besides, photocatalytic activity was also affected by calcination time (Fig. 7b), and it increased with calcination time increasing from 0.5 to 2 h. When calcination time was 2 h under 450 °C, PEG_{2000}-TiO_2 film showed the optimal degradation efficiency. In order to further optimize PEG_{2000}-TiO_2 film, different coating layers were investigated by degradation of Rh B, and the results were shown in Fig. 7c. 3-layer PEG_{2000}-TiO_2 film had the highest degradation efficiency, in comparison with 1-layer, 2-layer and 4-layer films. It may be ascribed to the appropriate thickness of film. Generally, the pathway of photocatalytic reaction is that Rh B molecule is firstly adsorbed on the solid-liquid interface of photocatalyst film prior to chemical reactions. While the photocatalyst film irradiated under light, reactive radicals could be generated and then Rh B molecule could be degraded by these photo-induced free radicals [40,41]. Therefore, 3-layer film with enough thickness could provide sufficient sites for adsorbing Rh B molecule resulting to its highest photocatalytic performance. However, thicker film (4-layer film in Fig. 7c) could block the light irradiation, which leaded to decrease of Rh B degradation efficiency. These results concluded that optimized PEG_{2000}-TiO_2 film was calcinated under 450 °C for 2 h with 3 layers. Importantly, optimized PEG_{2000}-TiO_2 film possessed much higher catalytic ability for Rh B degradation, compared with pure TiO_2 film (Fig. 8). After 60 min of irradiation, over 95.0% of Rh B was degraded by optimized PEG_{2000}-TiO_2 film, while only about 50.8% of Rh B was removed over pure TiO_2 film. Therefore, optimized PEG_{2000}-TiO_2 film could be used for further study to develop new photocatalytic system in this work.

3.4. Synergistic effect and mechanism of sonophotocatalysis using Photocatalytic-Ultrasonic system

It's reported that acoustic cavitation from sonolysis could lead to decomposition of water into hydroxyl ($OH^{\cdot}$), hydrogen ($H^{\cdot}$) and hydroperoxyl (HO_2) radicals [10,13], which have strong ability to degrade organic matters. These chemical reactions usually take place in three regions: the region inside the bubble cavity that formed during sonolysis, the region at bubble-liquid interface and in the liquid [42]. In sonophotocatalysis, organic solution is not only with photocatalyst irradiated under light but also excited by ultrasonic, so a synergistic effect of photocatalysis and sonocatalysis could enhance photocatalytic degradation of organic due to the highly reactive free radicals. In this part, photocatalytic processes were conducted by only using photocatalytic reactor in the circular Photocatalytic-Ultrasonic system (Fig. 1). During photocatalytic process, there was photocatalyst films coated glass beads in photocatalytic reactor, while uncoated glass beads in ultrasonic reactor. Sonocatalysis was investigated by using photocatalyst film in ultrasonic reactor, while in photocatalytic reactor there was uncoated glass beads without UV light. Sonophotocatalysis was carried out through Photocatalytic reactor under UV light and Ultrasonic reactor, respectively. In both reactors, there were photocatalyst films coated glass beads to degrade Rh B solution. Rh B was firstly through photocatalytic reactor and then flowed through ultrasonic reactor in this circular Photocatalytic-Ultrasonic system.

Comparison of photocatalysis, sonocatalysis and sonophotocatalysis were shown in Fig. 9. Both of photocatalytic reactor and

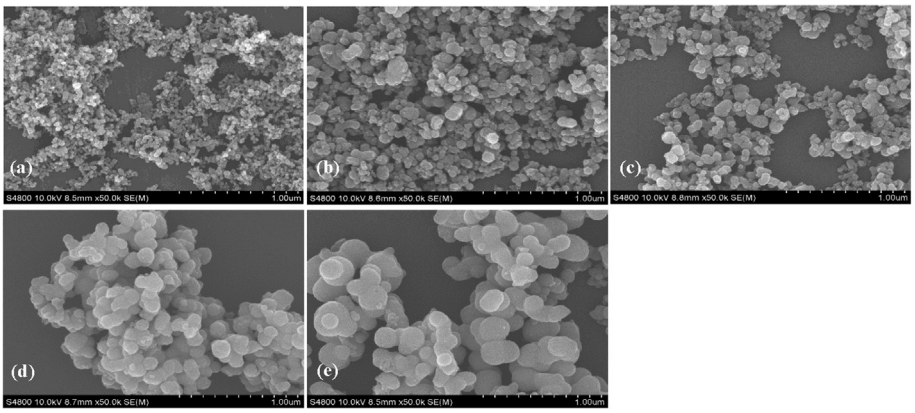

Fig. 4. SEM images of (a) Pure TiO_2, (b) PEG_{300}-TiO_2, (c) PEG_{2000}-TiO_2, (d) PEG_{6000}-TiO_2 and (e) PEG_{20000}-TiO_2 powders.

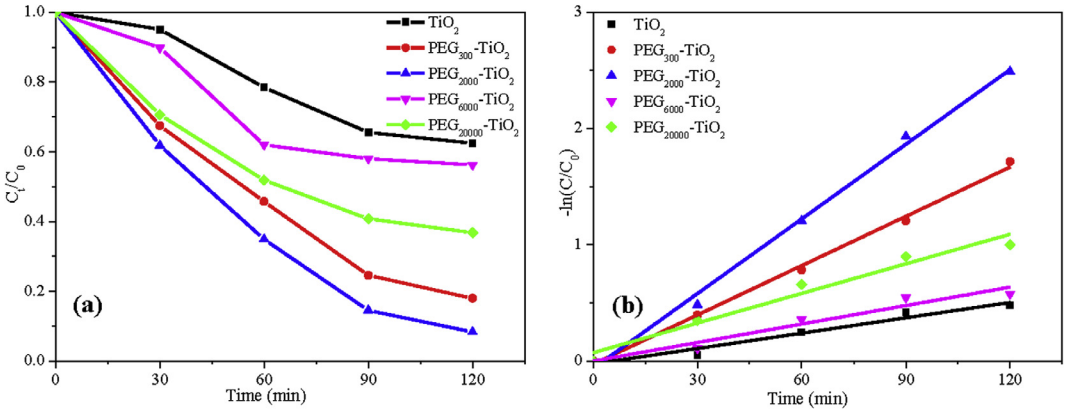

Fig. 5. (a) Photocatalytic degradation of Rh B solution, and (b) the pseudo-first-order kinetics by different PEG_{MW}-TiO_2 photocatalysts under UV light irradiation (Light intensity: 12.8 W/m^2, Rh B concentration: 2 mg/L).

Table 2
Pseudo first-order kinetic parameters of Rh B degradation by different photocatalysts.

	Pure TiO_2	PEG_{300}-TiO_2	PEG_{2000}-TiO_2	PEG_{6000}-TiO_2	PEG_{20000}-TiO_2
k_{app} (min^{-1})	0.00046	0.00083	0.00093	0.00049	0.00068
R^2	0.988	0.970	0.992	0.950	0.943

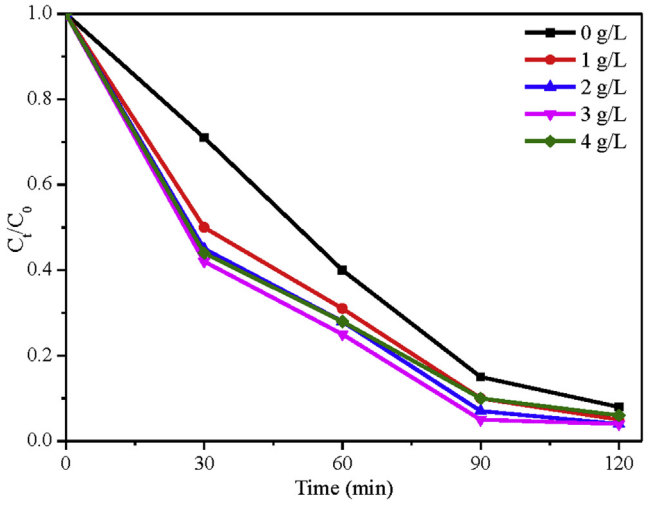

Fig. 6. Photocatalytic degradation of Rh B solution by PEG_{2000}-TiO_2 photocatalysts with different PEG addition levels under UV light irradiation (Light intensity: 12.8 W/m^2, Rh B concentration: 2 mg/L).

ultrasonic reactor were filled up with 2 g of glass beads, and ultrasound with 120 W was used for these experiments. The results indicated that PEG_{2000}-TiO_2 film without UV light irradiation or ultrasonic had the lowest ability for Rh B degradation, and only about 7.5% of Rh B were removed. Around 17.5% of Rh B were degraded after 120 min by sonocatalysis (PEG_{2000}-TiO_2 film, US), while 71.1% of Rh B were decolored by photocatalysis (PEG_{2000}-TiO_2 film, UV). Moreover, sonophotocatalysis (PEG_{2000}-TiO_2 film, US + UV) exhibited much higher efficiency than photocatalysis and sonocatalysis, and 97.2% Rh B molecule was decomposed in sonophotocatalysis. Interestingly, the combination of photocatalysis and sonocatalysis could lead to the synergistic effect. Reaction rate constant (k_{US+UV}) of sonophotocatalysis (0.0267 min^{-1}) was three times of photocatalysis (k_{UV} = 0.0088 min^{-1}), and fifty-three times of sonocatalysis (k_{US} = 0.0005 min^{-1}). Therefore, sonophotocatalytic effect was much higher than the sum of photocatalytic and sonocatalytic effects. The synergy between photocatalysis and sonocatalysis is usually quantified as the normalized difference between their rate constants in the presence of photocatalysts shown in Eq. (1) [14].

$$\text{Synergy} = \frac{k_{US+UV} - (k_{US}k_{UV})}{k_{US+UV}} \quad (1)$$

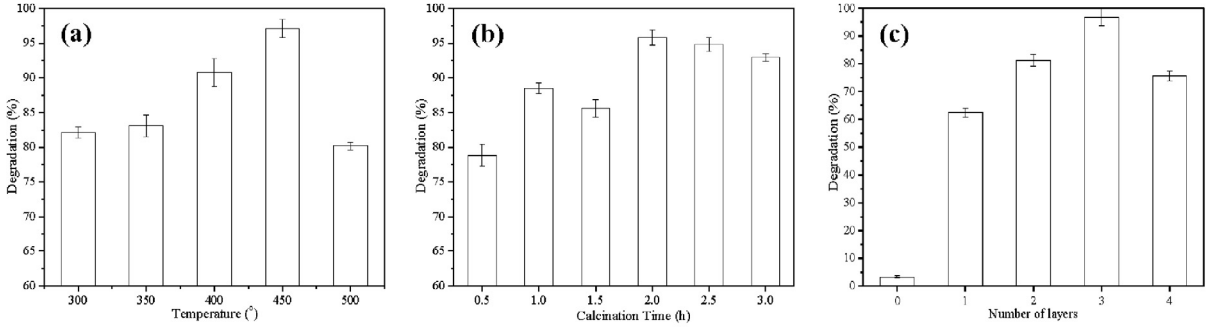

Fig. 7. Photocatalytic degradation of Rh B by PEG_{2000}-TiO_2 film coated glass beads under (a) different calcination temperature, (b) calcination time and (c) coating layers (Light intensity: 12.8 W/m^2, Time: 60 min).

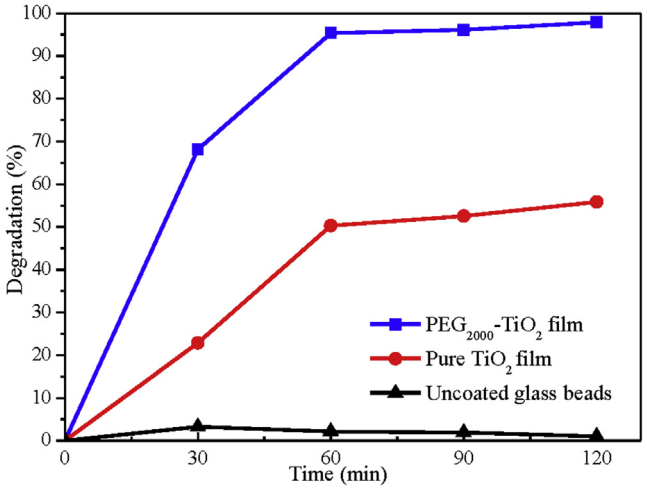

Fig. 8. Comparison of photocatalytic abilities of uncoated glass beads, TiO_2 film and optimized PEG_{2000}-TiO_2 film coated glass beads under UV light irradiation (Light intensity: 12.8 W/m^2).

The obtained synergy (0.6519) indicated the extremely high catalytic efficiency of this Photocatalytic-Ultrasonic system. Proposed mechanism is inferred in Fig. 10 that the presence of bubble cavitation leaded to the enhancement of generated free radical (·OH and H·) due to the localized temperatures and pressures. Besides, TiO_2 photocatalyst could be excited to generate not only superoxide radicals ($O_2^{\cdot-}$) on conduction band, but also form hydroxyl radicals (·OH) and holes on valence band [14]. These active species (·OH, H·, $O_2^{\cdot-}$ and holes) can directly oxidize organics. Therefore, the combination of photocatalysis and sonocatalysis could result in the great synergistic effect for photocatalytic degradation of organics.

To further investigate the parameters of ultrasonic on Rh B degradation, sonocatalysis by PEG_{2000}-TiO_2 film coated glass beads were conducted using different ultrasonic power (Fig. S1). Besides, sonocatalysis by PEG_{2000}-TiO_2 film coated glass beads, pure TiO_2 film coated glass beads and uncoated glass beads were compared in Photocatalytic-Ultrasonic system (Fig. S2), respectively. In these experiments, both of photocatalytic reactor and ultrasonic reactor were filled up with 4 g of glass beads, while ultrasound with 120 W was used in Fig. S2. The results indicated that the 120 W of ultrasonic power showed higher Rh B degradation efficiency (65.7%) than 30 W of ultrasonic power (61.1%). Besides, PEG_{2000}-TiO_2 film showed the higher sonocatalytic efficiency than pure TiO_2 film and uncoated glass beads. Sonocatalytic degradation ratio of Rh B by PEG_{2000}-TiO_2 film was 65.7% after 2 h in Fig. S2, which was higher than the sonocatalytic degradation ratio (17.5%) in Fig. 8, due to that the amount of PEG_{2000}-TiO_2 film coated glass beads (4 g) in ultrasonic reactor in Fig. S2 was twice of that in Fig. 8 (2 g). Therefore, larger amount of PEG_{2000}-TiO_2 coated glass beads, higher ultrasonic power and longer experimental time could contribute to higher degradation efficiency of Rh B.

In addition, repetitive experiments were conducted by sonophotocatalysis, and the results were shown in Fig. 11. It could be clearly found that the fifth circle experiment still possessed high photocatalytic activity, and still about 97.2% of Rh B were degraded using PEG_{2000}-TiO_2 film by sonophotocatalysis in this Photocatalytic-Ultrasonic system. This result indicated that PEG_{2000}-TiO_2 film not only had excellent catalytic activity but also showed high stability.

4. Conclusion

In summary, the circular Photocatalytic-Ultrasonic system was successfully developed and utilized for photocatalytic, sonocatalytic and sonophotocatalytic reaction in this work. PEG2000 modified TiO_2 calcinated under 450 °C for 2 h exhibited the smallest crystallite size, optimal particle size, higher specific surface area and the highest photocatalytic activity. The synergistic effect of ultrasonication and photocatalysis on PEG_{2000}-TiO_2 film in Photocatalytic-Ultrasonic system resulted to improved activity for Rh B degradation, which may be ascribed to the enhancement of generated free radicals. In addition, PEG_{2000}-TiO_2 film in this system possessed high photochemical stability even after five-repetitive operation for Rh B degradation. Due to its excellent activity and high stability, PEG_{2000}-TiO_2 film in this Photocatalytic-Ultrasonic system could be the potential candidate for wastewater treatment.

Acknowledgements

This work is supported by Grant-in-Aid for Exploratory Research 26670901 and Scientific Research (B) 15H02859 from Japan Society for the Promotion of Science (JSPS) in Japan.

Appendix A. Supplementary data

Supplementary data associated with this article can be found, in the online version, at http://dx.doi.org/10.1016/j.ultsonch.2016.12.008.

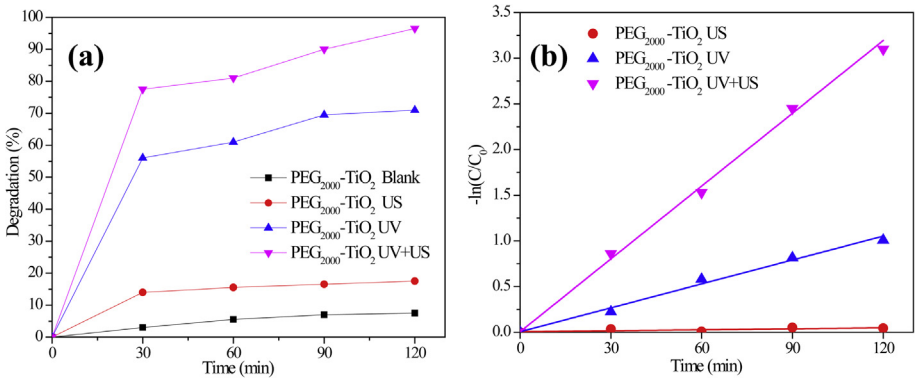

Fig. 9. Photocatalytic, sonocatalytic and sonophotocatalytic treatment for (a) Rh B degradation, and (b) the pseudo-first-order kinetics by optimized PEG_{2000}-TiO_2 film on glass beads using Photocatalytic-Ultrasonic system. Both of photocatalytic reactor and ultrasonic reactor were filled up with 2 g of glass beads. (Light intensity: 12.8 W/m^2, Ultrasonic: 120 W).

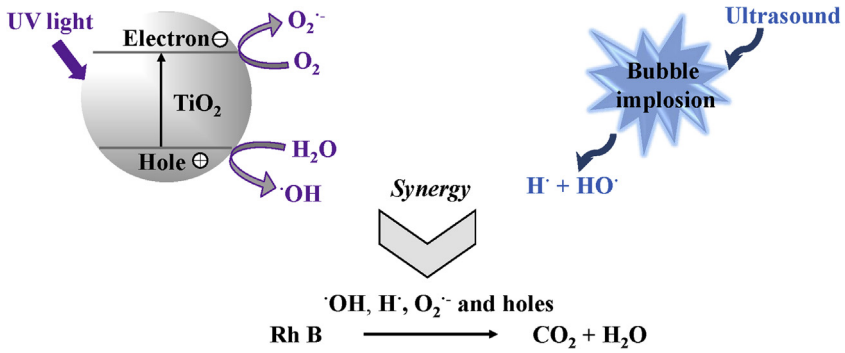

Fig. 10. Proposed mechanism of sonophotocatalysis for Rh B degradation using Photocatalytic-Ultrasonic system.

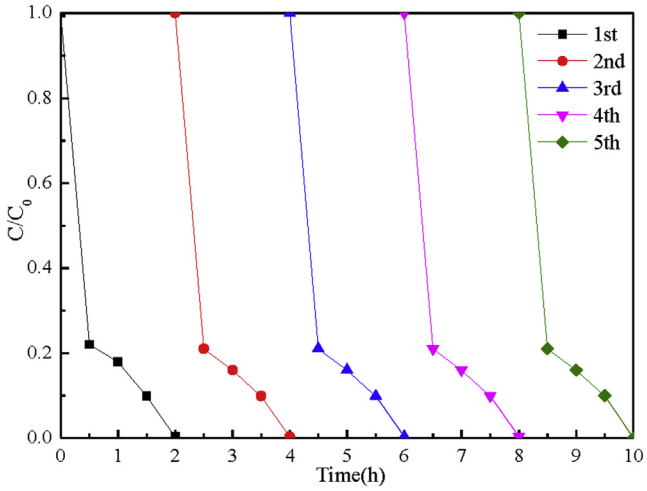

Fig. 11. Repetitive performance of optimized PEG_{2000}-TiO_2 film coated glass beads for Rh B degradation by sonophotocatalysis using Photocatalytic-Ultrasonic system. Both of photocatalytic reactor and ultrasonic reactor were filled up with 2 g of glass beads. (Light intensity: 12.8 W/m^2, Ultrasonic: 120 W).

References

[1] S.H.S. Chan, T. Yeong Wu, J.C. Juan, C.Y. Teh, Recent developments of metal oxide semiconductors as photocatalysts in advanced oxidation processes (AOPs) for treatment of dye waste-water, J. Chem. Technol. Biotechnol. 86 (2011) 1130–1158.

[2] A. Stasinakis, Use of selected advanced oxidation processes (AOPs) for wastewater treatment-a mini review, Global Nest J. 10 (2008) 376–385.

[3] K. Kestioğlu, T. Yonar, N. Azbar, Feasibility of physico-chemical treatment and advanced oxidation processes (AOPs) as a means of pretreatment of olive mill effluent (OME), Process Biochem. 40 (2005) 2409–2416.

[4] E.J. Hart, A. Henglein, Free radical and free atom reactions in the sonolysis of aqueous iodide and formate solutions, J. Phys. Chem. 89 (1985) 4342–4347.

[5] A.E. Alegria, Y. Lion, T. Kondo, P. Riesz, Sonolysis of aqueous surfactant solutions: probing the interfacial region of cavitation bubbles by spin trapping, J. Phys. Chem. 93 (1989) 4908–4913.

[6] V. Misik, N. Miyoshi, P. Riesz, EPR spin-trapping study of the sonolysis of H_2O/D_2O mixtures: probing the temperatures of cavitation regions, J. Phys. Chem. 99 (1995) 3605–3611.

[7] A.L. Prajapat, P. Das, P.R. Gogate, A novel approach for intensification of enzymatic depolymerization of carboxymethyl cellulose using ultrasonic and ultraviolet irradiations, Chem. Eng. J. 290 (2016) 391–399.

[8] V. Desai, M.A. Shenoy, P.R. Gogate, Degradation of polypropylene using ultrasound-induced acoustic cavitation, Chem. Eng. J. 140 (2008) 483–487.

[9] P. Riesz, D. Berdahl, C. Christman, Free radical generation by ultrasound in aqueous and nonaqueous solutions, Environ. Health Perspect. 64 (1985) 233.

[10] C.G. Joseph, G.L. Puma, A. Bono, D. Krishnaiah, Sonophotocatalysis in advanced oxidation process: a short review, Ultrason. Sonochem. 16 (2009) 583–589.

[11] S.C. Panchangam, A.Y.-C. Lin, J.-H. Tsai, C.-F. Lin, Sonication-assisted photocatalytic decomposition of perfluorooctanoic acid, Chemosphere 75 (2009) 654–660.

[12] C. Berberidou, I. Poulios, N. Xekoukoulotakis, D. Mantzavinos, Sonolytic, photocatalytic and sonophotocatalytic degradation of malachite green in aqueous solutions, Appl. Catal. B Environ. 74 (2007) 63–72.

[13] N.N. Mahamuni, Y.G. Adewuyi, Advanced oxidation processes (AOPs) involving ultrasound for waste water treatment: a review with emphasis on cost estimation, Ultrason. Sonochem. 17 (2010) 990–1003.

[14] M. Mrowetz, C. Pirola, E. Selli, Degradation of organic water pollutants through sonophotocatalysis in the presence of TiO_2, Ultrason. Sonochem. 10 (2003) 247–254.

[15] A. Fujishima, K. Honda, S. Kikuchi, Photosensitized electrolytic oxidation on semiconducting n-type TiO_2 electrode, Kogyo Kagaku Zasshi 72 (1969) 108–113.

[16] A. Fujishima, K. Honda, Electrochemical photolysis of water at a semiconductor electrode, Nature 238 (1972) 37–38.

[17] M.R. Hoffmann, S.T. Martin, W. Choi, D.W. Bahnemann, Environmental applications of semiconductor photocatalysis, Chem. Rev. 95 (1995) 69–96.

[18] D. Mardare, M. Tasca, M. Delibas, G. Rusu, On the structural properties and optical transmittance of TiO_2 rf sputtered thin films, Appl. Surf. Sci. 156 (2000) 200–206.

[19] W.G. Lee, S.I. Woo, J.C. Kim, S.H. Choi, K.H. Oh, Preparation and properties of amorphous TiO_2 thin films by plasma enhanced chemical vapor deposition, Thin Solid Films 237 (1994) 105–111.

[20] D. Byun, Y. Jin, B. Kim, J.K. Lee, D. Park, Photocatalytic TiO_2 deposition by chemical vapor deposition, J. Hazard. Mater. 73 (2000) 199–206.

[21] E. Halary, G. Benvenuti, F. Wagner, P. Hoffmann, Light induced chemical vapour deposition of titanium oxide thin films at room temperature, Appl. Surf. Sci. 154 (2000) 146–151.

[22] T. Nishide, F. Mizukami, Effect of ligands on crystal structures and optical properties of TiO_2 prepared by sol–gel processes, Thin Solid Films 353 (1999) 67–71.

[23] S. Zhang, Y. Zhu, D. Brodie, Photoconducting TiO_2 prepared by spray pyrolysis using $TiCl_4$, Thin Solid Films 213 (1992) 265–270.

[24] B. Guo, Z. Liu, L. Hong, H. Jiang, J.Y. Lee, Photocatalytic effect of the sol–gel derived nanoporous TiO_2 transparent thin films, Thin Solid Films 479 (2005) 310–315.

[25] Y. Djaoued, S. Badilescu, P. Ashrit, D. Bersani, P. Lottici, J. Robichaud, Study of anatase to rutile phase transition in nanocrystalline titania films, J. Sol–Gel Sci. Technol. 24 (2002) 255–264.

[26] M. Vong, N. Bazin, P. Sermon, Chemical modification of silica gels, J. Sol–Gel Sci. Technol. 8 (1997) 499–505.

[27] H.D. Jang, S.-K. Kim, S.-J. Kim, Effect of particle size and phase composition of titanium dioxide nanoparticles on the photocatalytic properties, J. Nanopart. Res. 3 (2001) 141–147.

[28] K. Kočí, L. Obalová, L. Matějová, D. Plachá, Z. Lacný, J. Jirkovský, O. Šolcová, Effect of TiO_2 particle size on the photocatalytic reduction of CO_2, Appl. Catal. B: Environ. 89 (2009) 494–502.

[29] G. Yang, Z. Jiang, H. Shi, T. Xiao, Z. Yan, Preparation of highly visible-light active N-doped TiO_2 photocatalyst, J. Mater. Chem. 20 (2010) 5301–5309.

[30] J.H. Park, S. Kim, A.J. Bard, Novel carbon-doped TiO_2 nanotube arrays with high aspect ratios for efficient solar water splitting, Nano Lett. 6 (2006) 24–28.

[31] Y. Zhang, C. Han, G. Zhang, D.D. Dionysiou, M.N. Nadagouda, PEG-assisted synthesis of crystal TiO_2 nanowires with high specific surface area for enhanced photocatalytic degradation of atrazine, Chem. Eng. J. 268 (2015) 170–179.

[32] Y. Takahashi, Y. Matsuoka, Dip-coating of TiO_2 films using a sol derived from Ti(O-i-Pr)$_4$-diethanolamine-H_2O-i-PrOH system, J. Mater. Sci. 23 (1988) 2259–2266.

[33] J. Byrne, B. Eggins, N. Brown, B. McKinney, M. Rouse, Immobilisation of TiO_2 powder for the treatment of polluted water, Appl. Catal. B: Environ. 17 (1998) 25–36.

[34] J. Sun, L. Jiao, X. Wei, W. Peng, L. Liu, H. Yuan, Effect of PEG molecular weight on the crystal structure and electrochemical performance of LiV_3O_8, J. Solid State Electron. 14 (2010) 615–619.

[35] H. Chang, E.-H. Jo, H.D. Jang, T.-O. Kim, Synthesis of PEG-modified TiO_2–$InVO_4$ nanoparticles via combustion method and photocatalytic degradation of methylene blue, Mater. Lett. 92 (2013) 202–205.

[36] X. Hu, Q. Zhu, X. Wang, N. Kawazoe, Y. Yang, Nonmetal–metal–semiconductor-promoted P/Ag/Ag_2O/Ag_3PO_4/TiO_2 photocatalyst with superior photocatalytic activity and stability, J. Mater. Chem. A 3 (2015) 17858–17865.
[37] S. Šegota, L. Ćurković, D. Ljubas, V. Svetličić, I.F. Houra, N. Tomašić, Synthesis, characterization and photocatalytic properties of sol–gel TiO_2 films, Ceram. Int. 37 (2011) 1153–1160.
[38] Á.A. Ramírez-Santos, P. Acevedo-Peña, E.M. Córdoba, Enhanced photocatalytic activity of TiO_2 films by modification with polyethylene glycol, Quim. Nova 35 (2012) 1931–1935.
[39] M. Feilizadeh, M. Vossoughi, S.M.E. Zakeri, M. Rahimi, Enhancement of efficient Ag–S/TiO_2 nanophotocatalyst for photocatalytic degradation under visible light, Ind. Eng. Chem. Res. 53 (2014) 9578–9586.
[40] G. Xue, H. Liu, Q. Chen, C. Hills, M. Tyrer, F. Innocent, Synergy between surface adsorption and photocatalysis during degradation of humic acid on TiO_2/activated carbon composites, J. Hazard. Mater. 186 (2011) 765–772.
[41] S. Liu, M. Li, S. Li, H. Li, L. Yan, Synthesis and adsorption/photocatalysis performance of pyrite FeS_2, Appl. Surf. Sci. 268 (2013) 213–217.
[42] Y.G. Adewuyi, Sonochemistry: environmental science and engineering applications, Ind. Eng. Chem. Res. 40 (2001) 4681–4715.